TECHNICAL PAPER

Experimental investigation of porous media combustion applied on the piston bowl of diesel engine

Subhasish Das[1] · Biplab Kumar Debnath[1] · Rajat Subhra Das[1]

Abstract

The attainment of homogenous combustion in diesel engines has always been a challenge. The erstwhile literatures reported the potential of porous media (PM) in enhancing the homogeneity of fuel–air mixture in various combustion devices. Taking cognisance of this fact, it was attempted to apply PM on the piston bowl of the diesel engine to study the consequent efficacy of homogenous combustion. It was revealed from the study that with the application of PM on the piston bowl, the evaporation rate of the fuel mixture was enhanced (shorter ignition delay) and mechanical efficiency was also improved as compared to the conventional engine. Compression tests were performed for the three commercially available PMs, like silicon carbide, alumina and zirconia, to determine their load bearing capacity inside the engine during operation. Silicon carbide was found to have better material strength to resist load. Also, experimental analysis was conducted by the use of cylindrical shaped silicon carbide fixed in the cylindrical piston bowl, which was modified from the traditional hemispherical one. The standard volumetric compression ratio of 17.5 and the porosity of ~ 78% were considered for PM. The experiments were performed at different part loads with PM for the safe operation of the engine. The mechanical efficiency (η_m) was found to enhance by ~ 9% and ignition delay got advanced by ~ 2° crank angle with PM. Emission parameters with PM, such as nitrogen oxides (NO_X) and carbon dioxide (CO_2) were reduced up to ~ 62% and ~ 39%, respectively, than those of conventional diesel engine.

✉ Biplab Kumar Debnath
  biplab.debnath@nitm.ac.in

  Subhasish Das
  subhasishdas42@gmail.com

  Rajat Subhra Das
  rajatsubhra@nitm.ac.in

1 Department of Mechanical Engineering, National Institute of Technology Meghalaya, Shillong, Meghalaya 793003, India

Graphic abstract

Experimental Results
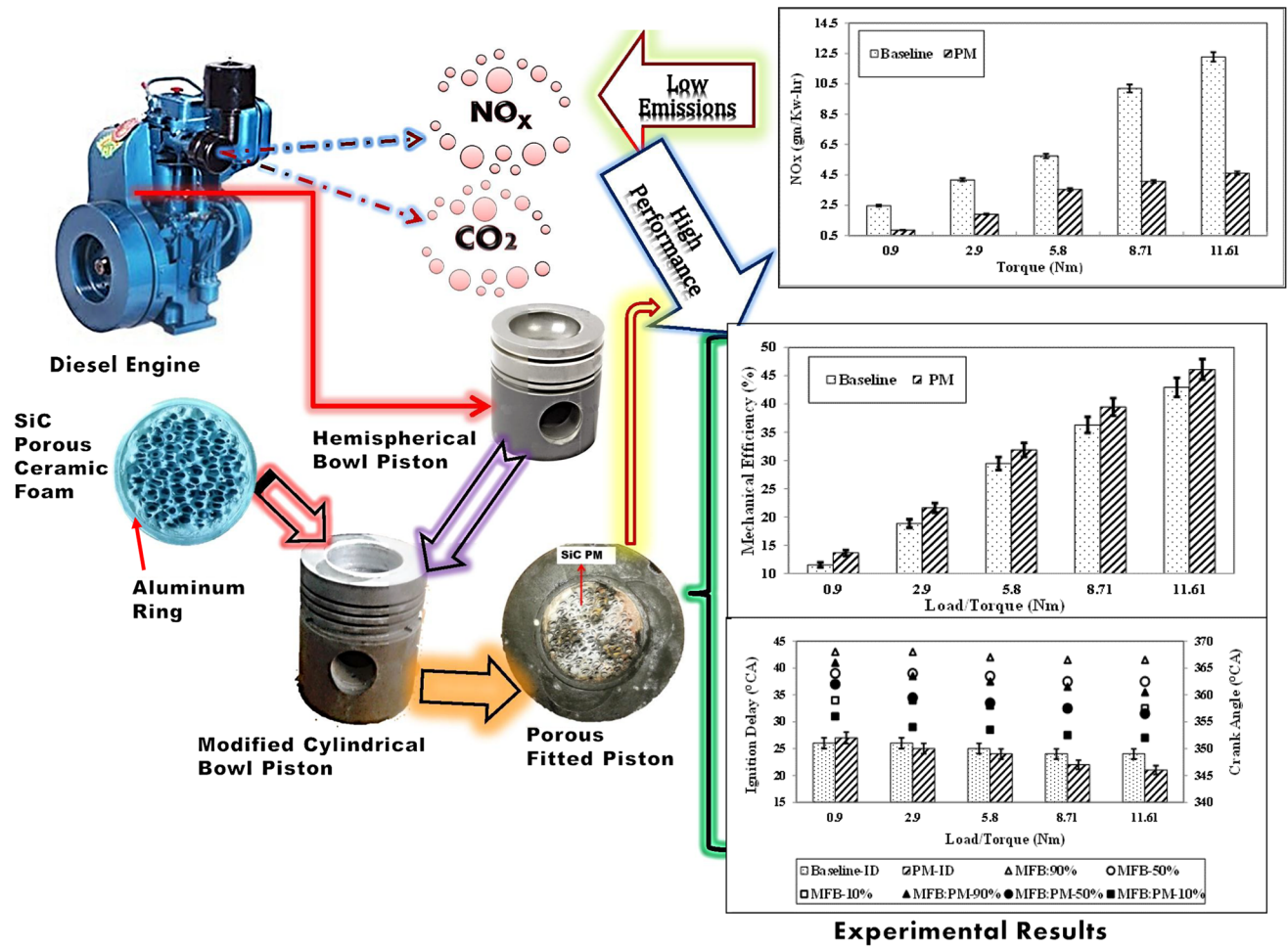
Keywords Modified piston bowl · Porous media · Compression test · Mechanical efficiency · Emissions

Abbreviations

3D	Three-dimensional
Al_2O_3	Alumina
BP	Brake power (kW)
BTDC	Before top dead center (°)
BTHE	Brake thermal efficiency (%)
CA	Crank angle (°)
CFD	Computational fluid dynamics
CO	Carbon monoxide (ppm)
CO_2	Carbon dioxide (%)
CR	Compression ratio
EGR	Exhaust gas recirculation
HC	Hydrocarbon
HRR	Heat release rate (J/°)
ID	Ignition delay (°)
IP	Indicated power (kW)
NO	Nitric oxide (ppm)

NO_2	Nitrogen dioxide (ppm)
NO_X	Nitrogen oxides (ppm)
PM	Porous media
SiC	Silicon carbide
UTM	Universal testing machine
ZrO_2	Zirconia

List of symbols

C_p	Specific heat (J/kg-K)
d_m	Mean pore diameter (mm)
k	Effective thermal conductivity (W/m-K)
Pe	Peclet number
S_L	Laminar flame speed (m/s)

Greek symbols

η_m	Mechanical efficiency (%)
ρ	Density (kg/m³)

1 Introduction

Diesel engine occupies a major global market due to its high power delivery, rigid structure, higher brake thermal efficiency (BTHE), as well as fuel economy; in comparison with the gasoline engines [1]. Low specific fuel consumption and high emission levels are the traits of compression ignition engines. Several methods such as exhaust gas recirculation (EGR), catalytic converter water injection and water-diesel emulsified fuel have been introduced to reduce the level of emissions as it poses a serious threat to the environment and human health [2, 3]. The use of reciprocating porous media (PM) as a regenerator inside the cylinder of diesel engines has been identified as a potential substitute for reducing fuel consumption along with polluting emissions such as nitrogen oxides (NO_X), hydrocarbons (HC), carbon monoxide (CO), and smoke. The thermal efficiency is found to be improved with PM compared to the conventional diesel engines [4].

The salient features of PM combustion include the attainment of high radiant output, high speed of the flame, higher density of power and modulation along with low NO_X and CO emissions. The major difference between the conventional combustion systems and PM is that it improves the effective transport of energy from the burnt mixture to the unburned one [5]. PM assists toward homogenous combustion inside the cylinder by instant release of energy in the whole region of PM matrix through consistent distribution of temperature due to the three-dimensional (3D) ignition [6]. The unique changes in the mass transfer characteristics through the 3D topology of the PM and heat recuperation permit appropriate mixing, which results in charge homogenization inside the PM [6]. In PM combustion, the quenching of the flame is described by a modified Peclet number (*Pe*), given in Eq. (1) [7, 8].

$$Pe = \frac{S_L d_m C_p \rho}{k} \tag{1}$$

The modified Pe defines the ratio between the discharge of energy owing to the ignition in a PM cavity and the quantity of energy escaped through the cavity walls. Moreover, it pronounces the ratio of the characteristic diameter of the PM cavity to the thickness of the front of laminar flame [6]. As reported by Trimis and Wawrzinek (2004), the spread of flame in PM is hardly hindered if Pe 65 ± 45 [8]. Ignition process is the significant aspect for a PM, in connection with the homogeneous combustion in an engine. Out of the total of four ignition methods (a) local ignition by the spark plug, (b) thermal self-ignition by compression, (c) controlled (low-temperature chemical) auto-ignition, and (d)

3D thermal PM self-ignition, the succeeding three methods can deliver a homogeneous combustion process [6].

Porous burner has proved to be a very promising technology in enhancing the combustion efficiency and minimizing the formation of pollutants [9]. Based on this encouraging feature of porous burner, the feasibility of achieving homogeneous combustion in diesel engine with PM (SiC) on cylinder head was experimentally evaluated by Durst and Weclas [10]. Their attempt proved to be successful, resulting in the decrement of emission, enhanced efficacy of the cycle and reduction in the noise of combustion to that of a traditional diesel engine. However, they did not report the in-cylinder analysis of combustion, such as pressure rise rate, heat release rate (HRR), mass fraction burnt, and ignition delay. Hall and Paroutka performed experimental analysis of the combustion stability with a conventional fuel injector. Using it, they injected methanol fuel inside the PM made burner [11]. They considered various combinations of flow rates of air and fuel to obtain steady combustion. Within the range of equivalence ratio of 0.2 to 0.65, they reported stable combustion. However, they could not achieve complete combustion of methanol under all conditions, especially when non-premixed (diffusion) flames were released downstream of the ceramic. Reijenders and his associates carried out experimental and numerical investigations on porous nozzle [12]. The investigation revealed the advantage that porous nozzle spray can provide a homogenous mixture of fuel and air. Also, they reported that the ignition delay was shorter for PM injector compared to the conventional one. The influence of the properties of PM on the characteristics of fuel injection, splitting effects of multi-jets and features of spray in a stainless constant volume chamber was studied experimentally by Shaahangian et al. [13]. According to them, in the presence of PM, the rich core zone of the spray reduces. Additionally, in the presence of PM, improved interaction between air and fuel was noticed at different fuel injection pressures. This is a significant factor for combustion efficacy.

The inference from the literatures revealed the influences of PM on the combustion behavior in diesel engines by applying it at the stationary components, such as, cylinder head and fuel injector. The performance effects due to the to-and-from motion of the engine's dynamic components, namely, the piston, in which PM is fixed on the modified bowl, are yet to be investigated. In the present work, experimental analysis was performed with PM fixed on the modified piston bowl (cylindrical shape) by considering performance, combustion and emission parameters. These parameters are compared with the conventional diesel engine parameters to evaluate the advantage of using PM towards engine application. All the experiments are performed for the load variations, represented as torque

Table 1 The thermo-physical properties of the PMs [10, 14]

Properties	Materials		
	SiC	Al_2O_3	ZrO_2
Maximum permissible temperature in air (°C)	1600	1900	1800
Thermal expansion coefficient (20–1000 °C) (10^{-6}/K)	4–5	8	10–13
Thermal conductivity (1000 °C) (W/m-K)	20–50	5–6	2–4
Total emissivity (2000 K)	0.9	0.28	0.31

Fig. 1 Images of porous structure of **a** SiC, **b** Al_2O_3, **c** ZrO_2

(a)   (b)   (c)
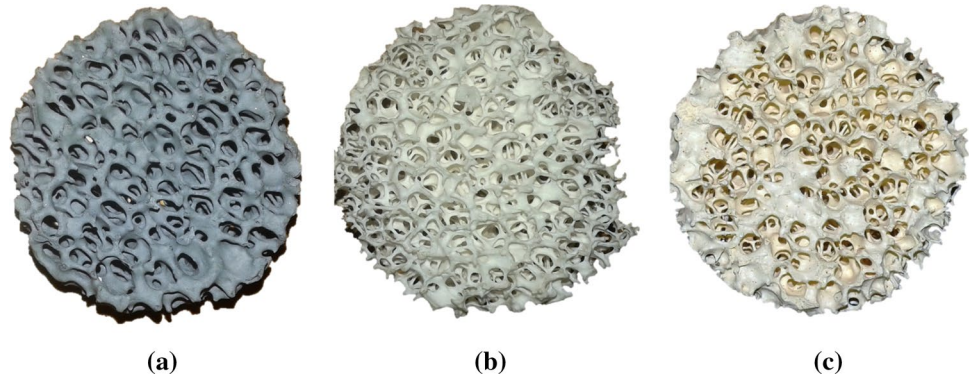
from 0.5 kg (0.90Nm) or No load to 6.4 kg (11.61Nm) in five steps.

2 Experimental methodology

2.1 Compression test of PMs

The high-pressure environment inside the combustion chamber raises the concern regarding the tolerance of PM to withstand it. So, before putting the PM inside the engine, compression tests of different PMs were performed in a hydraulic universal testing machine (UTM). This is done to find the material load bearing capacity, during engine operation. The selection of the PMs for the application in diesel engine is based on the favorable thermo-physical properties shown in Table 1 [10, 14]. The PMs, namely SiC, Al_2O_3 and ZrO_2, are procured from Eltech ceramics, Coimbatore, India, and presented in Fig. 1a–c [15]. The PMs are cylindrical in shape, and the dimensions are customized in accordance with the modified piston bowl dimension, which is cylindrical in shape (diameter = 52 mm and height = 22 mm).

2.2 Compressiontest in hydraulic universal testing machine (UTM)

As ceramic PMs are brittle in nature and fail in shear, the compression tests were performed, where it can provide the limit of load that the PM can sustain inside a compression ignition engine during its actual operation.

Table 2 UTM specifications (BSUT-100-JD)

Specifications	Values
Maximum capacity (kN)	1000
Load range with accuracy of measurement ± 1% (kN)	20–1000
Resolution of piston movement (displacement) (mm)	0.01
Tensile testing space (mm)	80–850
Compression space (mm)	0–765
Clearance between columns (mm)	710
Piston stroke (mm)	250
Crosshead moving speed (mm/min)	0–80
Power (kW)	2.2, 415/380 V, 3ph
Load frame (L×W×H) (mm)	980×650×2500
Clamping jaws for flat specimens of diameters (mm)	13–35, 35–55
Clamping jaws for flat specimens of thickness (mm)	0–40
Width (mm)	82
Pair of compression plate of diameter (mm)	205×205×30
Roller diameter (mm)	50
Maximum clearance between supports (mm)	700(ϕ 20)
Radius of punch tops (mm)	30

The compression tests showed that the specimen fractures because of the bulging action with compression loading and material crumbling. The specifications of the UTM are mentioned in Table 2. The compression tests are performed for different PMs, namely SiC, Al_2O_3 and ZrO_2. Load vs. displacement and stress vs. strain curves are

taken into consideration for the analysis, and the results obtained from the compression test are presented in results and discussion section.

Moreover, from the earlier study performed using computational fluid dynamics (CFD) by the same group of authors, and from the literatures, SiC was found suitable for engine application [16]. This is because the use of SiC showed higher peak cylinder temperature with a shorter ignition delay comparable to Al_2O_3 and ZrO_2. This is an indication of the combustion homogenization as desired from PM [10]. Hence, experimentation was performed with SiC. Thereafter, this PM has been fitted on the cylindrical piston bowl, modified from the conventional hemispherical one. This is because PM is commercially available in cylindrical shape. The diameter of the cylindrical piston bowl of 52 mm is the same to that of the hemispherical piston bowl of the conventional compression ignition engine. This bowl height of 22 mm is the maximum permissible modification limit in the piston bowl, as beyond this the piston bowl may rupture. Based on the dimension of the cylindrical piston bowl, the porosity of the PM is calculated as ~78% ("Appendix"). This porosity is required to retain the CR of 17.5 of the conventional compression ignition engine.

The SiC foam is customized to have a diametric tolerance of 2 mm (i.e., diameter ~50 mm) with a height of 22 mm. This is considered from the actual dimensions of the piston bowl available in the diesel engine. The circumference of the PM is covered by an aluminum ring (Fig. 2), to mount and lock it on the piston bowl.

2.3 Compression ignition engine experimental test rig

A 3.2-kW diesel engine (make: Kirloskar) coupled with an eddy-current-type, water-cooled dynamometer is used for the experiments. A panel box constitutes air box, fuel tank,
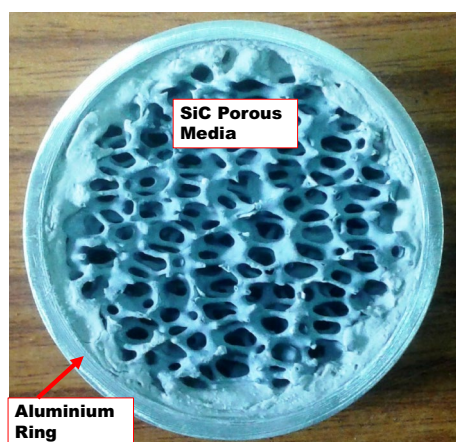

Fig. 2 SiC attached with aluminum ring

display for measurement of temperature, rpm, and load control knob. To control the flow of cooling water in the test rig and calorimeter, two rotameters are also fitted [17]. The specifications of the diesel engine and the data acquisition rate are summarized in Tables 3 and 4. The schematic diagram of the engine set up is shown in Fig. 3. The engine-out emissions, namely NO_X and carbon dioxide (CO_2), released through the exhaust pipe of the engine are measured using TESTO 350 flue gas analyzer. The specifications of the flue gas analyzer are mentioned in Table 5.

2.4 Experimental procedure

The experimental procedure was initiated with the dismantling of the engine component from the engine head to the connecting rod of the piston at the bottom. The modification of the piston bowl from the hemispherical one (Fig. 4) to the cylindrical one was performed to accommodate the cylindrical PM, commercially available as shown in Fig. 1. This dismantling was done to fit the PM (SiC) on the modified piston bowl (cylindrical) as shown in Fig. 5.

Before fitting the PM to the cylindrical piston bowl, high-temperature ceramic glue, named Zircon [19], was applied to the circumference of the aluminium ring of the PM. This is because during the engine operation, the rigorous dynamic motion of the piston may displace the PM from the bowl. This may break the PM and create damage in the engine. The PM is attached on the cylindrical piston bowl as shown in Fig. 6, by the process of press fitting on the lathe. Thereafter, the entire piston with PM is put inside an electric furnace (VFI 1400) for curing of the ceramic glue. The modified

Table 3 Specifications of the engine

Parameter	Specification
Make	Kirloskar
Type	1 cylinder, diesel,4-stroke, water-cooled
Rated power (kW), speed (rpm)	3.5, 1500
Cylinder diameter (mm), volumetric displacement (cm^3)	87.5, 661
Compression ratio (CR)	17.5
Stroke (mm)	110
Injection timing (°BTDC)	23
Injection Pressure (bar)	200
Dynamometer	Eddy current type, 0–12 kg, 185 mm radius
Temperature sensors	PT100, K type

Table 4 Data acquisition rate [18]

Parameter	Specification
Fuel flow meter	DP transmitter, range 0–500 mm WC
Air flow transmitter	Pressure transmitter (-) 250 mm WC
Pressure sensors	Piezo-type, range 5000 PSI, with low noise cable
Temperature sensors and transmitter	PT 100 (RTD) type, range 0–100 °C, output 4–20 mA (4 nos) K (ungrounded) type, range 0–1200 °C, output 4–20 mA (2 nos)
Load sensor and indicator	Strain gauge type load cell with digital indicator, range 0–50 kg
Speed sensor and indicator	Resolution 1°CA, range (5500 rpm) with TDC pulse
Data acquisition device	NI USB -6210, 16 bit, 250 kS/s
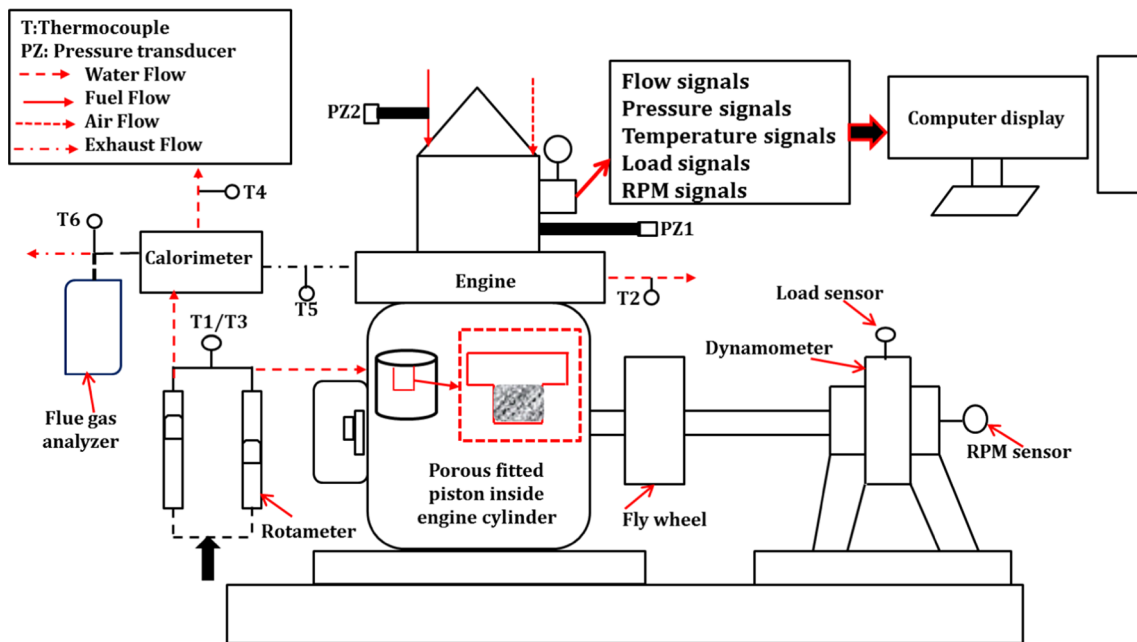
Fig. 3 Schematic diagram of the diesel engine test bench

Table 5 Specifications of the flue gas analyzer

Parameter	Resolution	Accuracy	Range
CO_2	0.01 Vol. % (0–25 Vol.%), 0.1 Vol.% (> 25 Vol. %)	± 0.3%Vol. % ± 1% of reading, (0–25 Vol. %), ± 0.5Vol.% ± 1.5% of reading (rest of range)	0–50 vol.%
NO	1 ppm	± 5 ppm (0-99 ppm) ± 5% of reading (100–1999.9 ppm) ± 10% of reading (rest of range)	0–4000 ppm
NO_2	0.1 ppm	± 5 ppm (0–99.9 ppm) ± 5% of reading (rest of range)	0–500 ppm
HC	1 ppm	400 ppm < 4000 ppm	0–40,000 ppm

piston is then reassembled in the engine, along with all the components to perform experiments with PM.

The PM-fitted engine was run with diesel fuel as per the baseline settings of CR 17.5 and fuel injection timing of 23 degree before top dead center (°BTDC), at a constant speed of 1500 ± 50 rpm. As SiC is brittle in nature, hence, for the safe operation of the engine, the experiment was performed at different part loads. The load variations represented as torque are 0.90 (No load), 2.90, 5.80, 8.71 and 11.61 Nm. The baseline tests of the engine with diesel fuel, in the presence of conventional hemispherical piston, are also performed at the standard settings. The load

Fig. 4 Hemispherical piston bowl

Fig. 5 Cylindrical piston bowl

variations considered are equal to those of the PM settings for comparing the performance of the engine with the baseline data. At each load, different parameters, namely, combustion and fuel pressures with respect to CA variations, temperatures, air, and fuel flow rate, speed, were recorded at least for three cycles from the experiments with baseline and PM and averaged at a particular load for analysis. Based on this, performance along with combustion analysis was performed with baseline and PM. Emission parameters, namely NO_X and CO_2, were also recorded
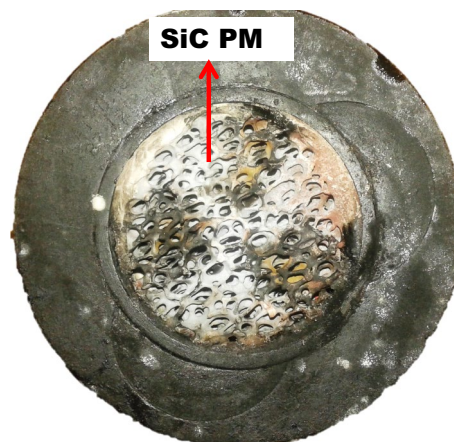
Fig. 6 PM-fitted piston

from the flue gas analyzer for both, baseline and with PM. The samples of flue gases were flown through the probe, once the engine reached steady-state. All the experiments were performed at 25 ± 2 °C and atmospheric condition.

3 Results and discussion

As stated in the experimental methodology section, the outcome of the compression tests performed for SiC, Al_2O_3 and ZrO_2 is presented first. Also, the results obtained from the experimentation for baseline test and PM are discussed. The results of performance, ignition delay (ID) and emissions are shown with load variation. The findings of combustion analysis are reported with the variation of CA.

3.1 Compression tests outcome

The compression test was performed in UTM. Initially, the load was applied gradually by displacing the head on the surface of SiC. After reaching maximum load of 15.03 kN at displacement of 1.9 mm, the material crosses its limit to withstand the load and the material fracture starts (Fig. 7). Similarly, for Al_2O_3 and ZrO_2, the maximum load, at which the material started to fracture was 14.54 kN and 15.49 kN, respectively. The displacement of load in Al_2O_3 was 1.3 mm, which is less as compared to SiC. The displacement for ZrO_2 was 0.9 mm, which is lesser than SiC and Al_2O_3. Although ZrO_2 withstood a little higher load than SiC, its rupture occurred 1 mm earlier than SiC. Therefore, it can be understood that SiC can withstand load for longer period as compared to ZrO_2 and Al_2O_3. The material failures for Al_2O_3 and ZrO_2 are also shown in Fig. 7. The stress vs strain curve is shown in Fig. 8. This curve shows that SiC has better material strength to resist load in comparison with Al_2O_3 and ZrO_2. The range of values of stress for Al_2O_3 and ZrO_2
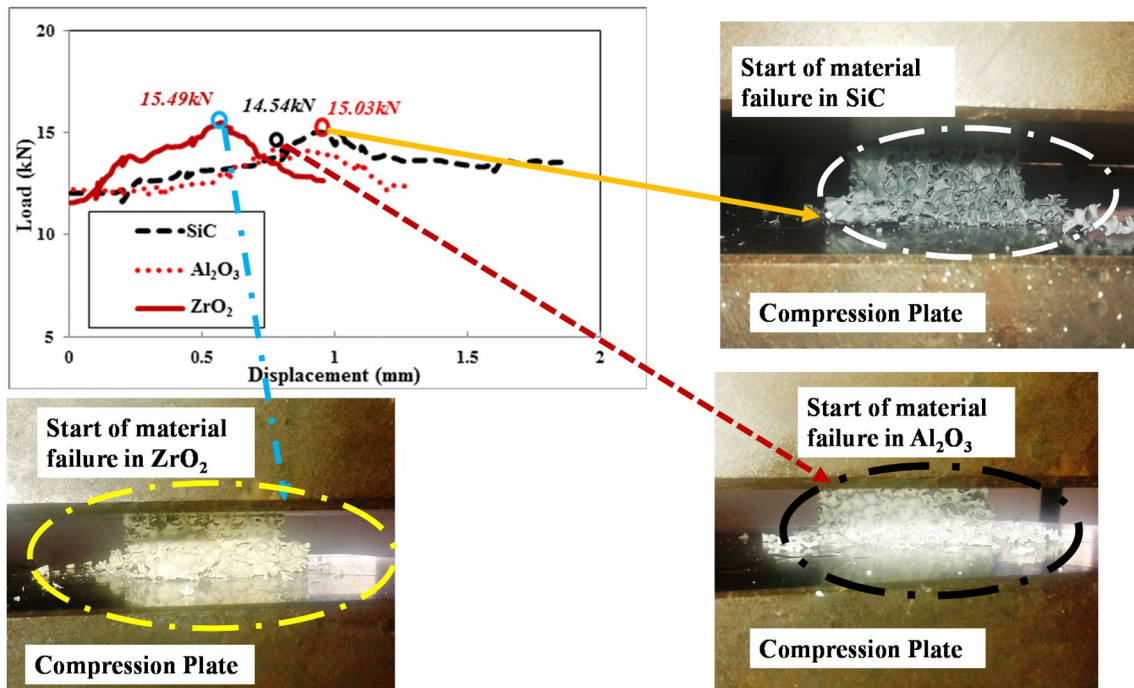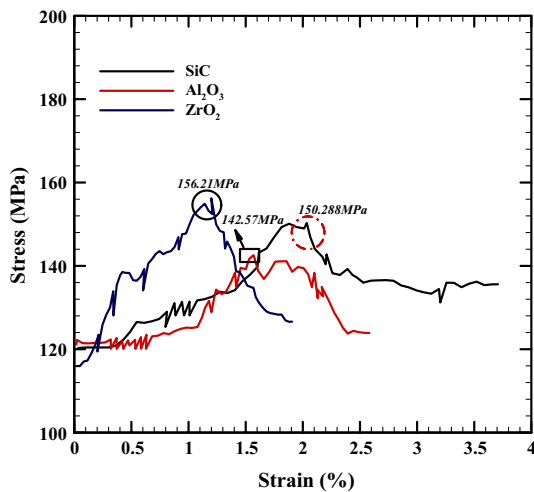
Fig. 7 Material failure in SiC, Al$_2$O$_3$ and ZrO$_2$

Fig. 8 Stress–strain curve of different PMs

Fig. 9 Variation of BTHE with load

is well within the permissible limit reported in the literature [20]. This is also validated based on the thermo-physical properties of PMs (Table 1). Although SiC has a little lower melting point (yet sufficient for diesel engine combustion) and lower thermal expansion coefficient, it has reasonably higher thermal conductivity, as well as higher emissivity. It implies that SiC can transfer heat more quickly to the piston material than other PMs and hence the piston will experience less thermal stress zone. The absorbed heat will be emitted at a faster rate from the surface of SiC due to higher emissivity [21].
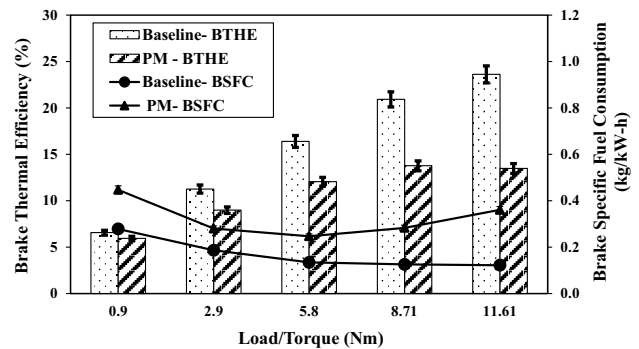
3.2 Performance analysis

The parameters that are used to evaluate the engine performance are BTHE and mechanical efficiency (η_m). The variations of BTHE at part loads for baseline and PM are shown in Fig. 9. BTHE is defined as the ratio of BP (net power obtained at the output of the crankshaft considering frictional loss) and the product of fuel consumption and calorific value [22].

It is seen from Fig. 9 that both for baseline and with PM, BTHE increases with the increase in load. But BTHE is found to be lower in PM than in baseline test. This indicates that fuel consumption in PM mode is a bit higher than in the conventional engine. BTHE signifies the conversion of the amount of heat generated from fuel
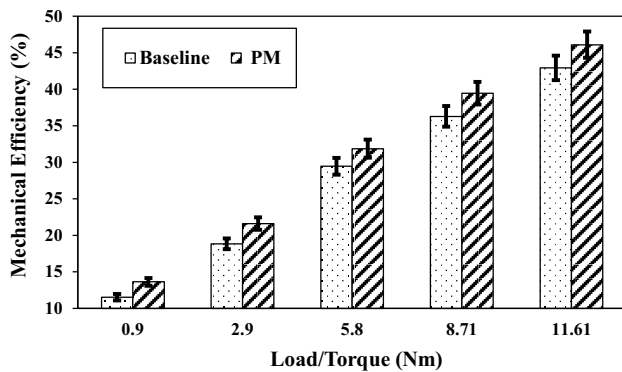
Fig. 10 Variation of η_m with load

Table 6 Peak cylinder pressure variation with load

Torque (Nm)	Peak cylinder pressure (bar)	
	Baseline	PM
0.9	45.98	39.23
2.90	47.47	43.32
5.80	48.49	44.70
8.71	52.66	46.72
11.61	54.77	50.21

to mechanical energy, i.e., work output. In PM, due to the rich fuel region, the entire fuel quantity may not get combusted and hence the energy conversion is lesser. Further, the regeneration effect in PM that carries away some amount of heat, generated from the combustion of fuel, may result in lowering the BTHE [4].

The performance of a system is determined in terms of efficiency. In the present work, the comparisons of the performance with baseline and PM are also measured in terms of η_m. It is defined as the ratio of the delivered BP to the indicated power (IP) [23]. Figure 10 depicts the increment of η_m with load for PM, to that of baseline test. The average increment of η_m at the loads of 0.90, 2.90, 5.80, 8.71, and 11.61 Nm for PM are 13.64, 21.62, 31.87, 39.47, and 46.11%, respectively, to that of baseline results of 11.53, 18.85, 29.47, 36.3, 42.94%, respectively. This increment in η_m for PM represents the reduction in heat energy loss apart from mechanical loss, which is a very significant factor in engine performance. Also, an earlier CFD study by the same authors reveals that the turbulent kinetic energy, which is important phenomenon in realising efficient combustion, is found to be augmented with PM, leading to generation of higher thermal energy [24]. The thermal energy recuperation [4] effect in PM avails enhanced energy efficiency as compared to the baseline run.

3.3 Combustion analysis

The results of combustion analysis with baseline test and PM are presented for the variation of average cylinder pressure, pressure rise rate, HRR and ignition delay (ID) at different part loads. The variations of average cylinder pressure inside the engine decode the combustion behavior. Till date, no literature reported the variation of pressure with respect to CA ($P - \theta$) for PM combustion in an internal combustion engine. With the increase in the load, the peak cylinder pressure increases (Table 6). This is because the mass flow rate of fuel is increased with the increase in load, resulting in

higher heat generation. The cylinder pressure variations at different loads with baseline and PM are shown in Fig. 11.

Along with Table 6, it reports that the average cylinder pressure is lower for PM than in baseline test. The drops in the peak pressure are reported as 6.75, 4.15, 3.79, 5.94, and 4.56 bar, at respective loads tested. This drop in pressure variation with PM is attributed to the inertial and viscous resistance of PM. The effect of viscous resistance results in controlled pressure variation in PM and with inertial resistance the gas mixture density decreases, which may lead to higher frictional losses [24]. The peak pressure developed, power produced and the smoothness with which the gas forces produced during combustion are transmitted to the piston are influenced by the rate of pressure rise in the engine combustion [22]. The variations of the pressure rise rate with CA at different loads are plotted in Fig. 12. It is observed from the plot that at 0.9 Nm, the pressure rise rate is lower in PM than that of baseline test. Also, the fuel is ignited a little earlier baseline test than with PM. This is because at a lower load, sufficient amount of energy is not stored in PM to assist in rapid evaporation of the fuel. Consequently, at 2.90Nm and 5.80Nm, the rate of pressure rise is greater with PM than the engine run in baseline mode. This is due to the release of stored energy from the earlier cycle with PM, which accounts for the regeneration of heat.

It is also observed that the ignition point is advanced for PM in both the loads and subsequently observed for 8.71Nm and 11.61 Nm. This leads to a relative earlier ignition of the premixed charge and rapid evaporation of fuel resulting in shorter ignition delay. Therefore, the accumulation of fuel is lesser in the combustion chamber. These results in a reduction in pressure rise rate at 8.71Nm and 11.61Nm [25]. From Fig. 12, it is seen that at 8.71Nm and 11.61Nm, the pressure rise rate is lowered with PM than in baseline test, which accounts for the effect of the viscous and the inertial resistances. The ignition delay accounts for the duration between fuel injection and fuel ignition [21]. The variation of ignition delay with fuel injection timing along with mass fraction burnt for 10%, 50%, and 90% with load is presented in Fig. 13. The values of peak rate of pressure rise and the CAs of combustion initiation for baseline and PM at different loads are illustrated in Table 7.
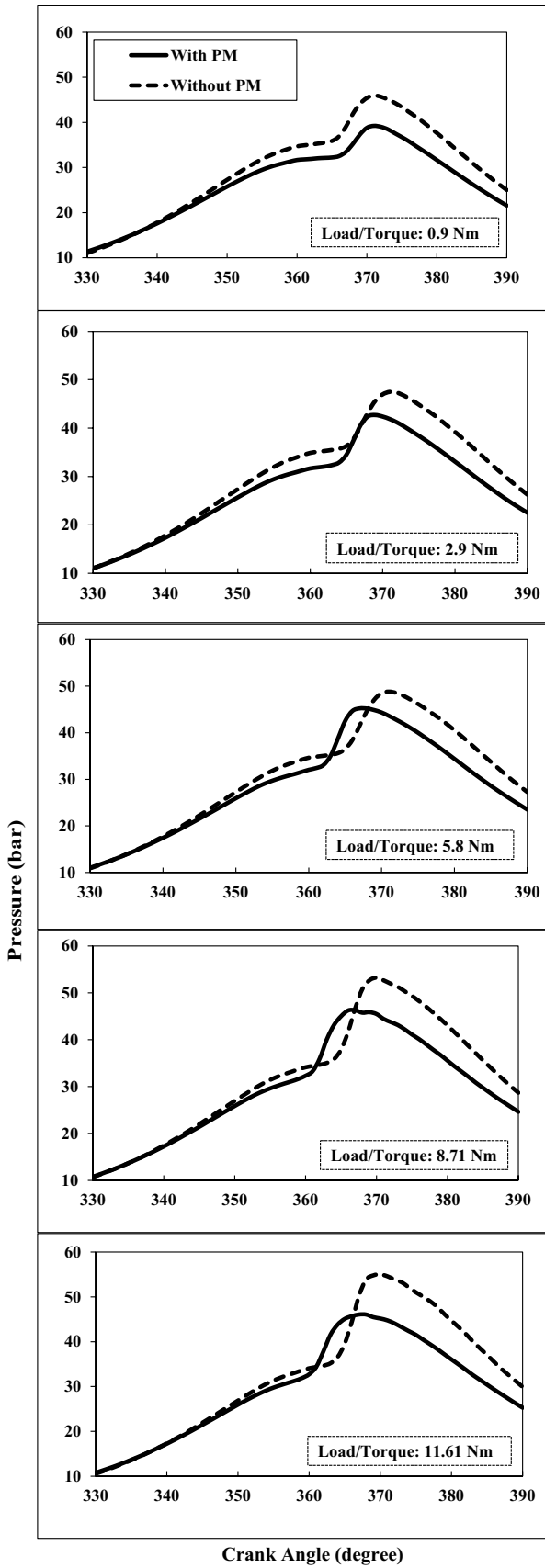
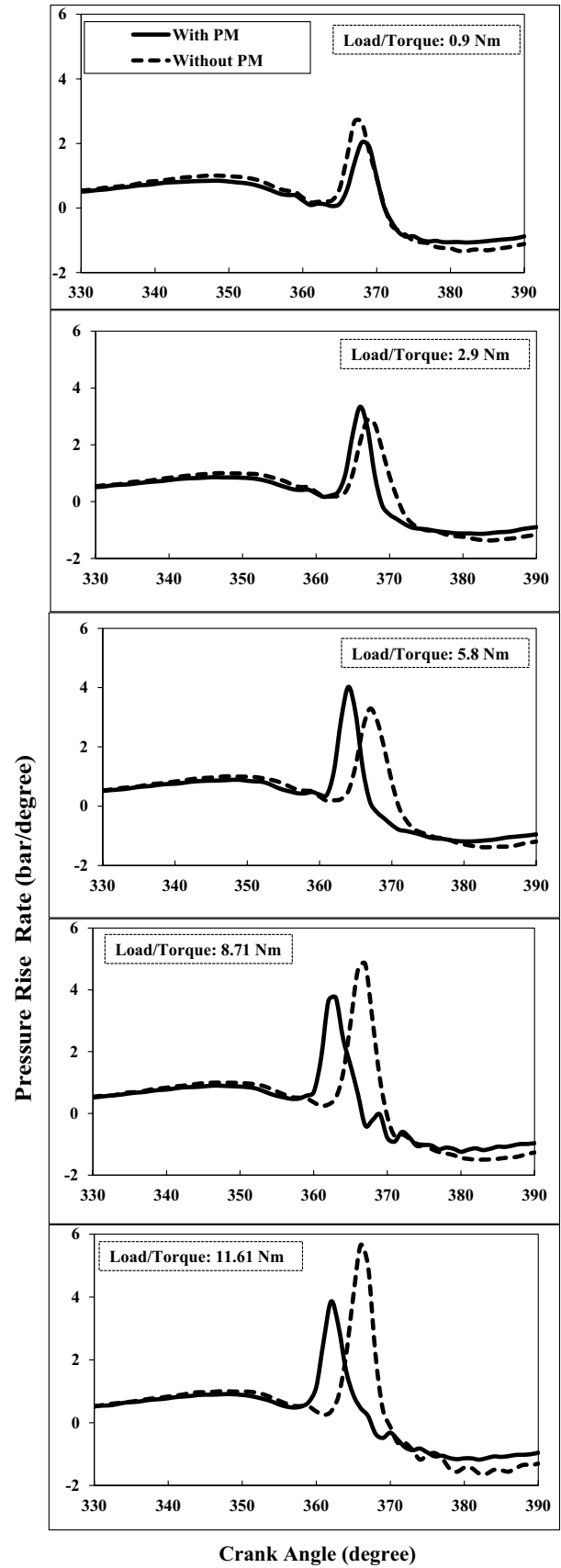**Fig. 11** Variation of cylinder pressure with CA at part load

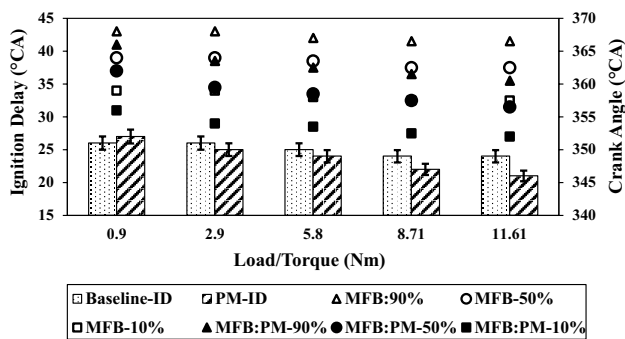**Fig. 12** Variation of rate of pressure rise with CA at part load

Fig. 13 Variation of ignition delays ("Injection Timing" 23°BTDC) and MFB at 10%, 50%, 90% with load

Table 7 Peak rate of pressure rise variation and CAs of combustion initiation

Sl. no	Torque (Nm)	Peak rate of pressure rise (bar/°)		Combustion initiation (°CA)	
		Baseline	PM	Baseline	PM
1	0.9	2.67	2.03	363	364
2	2.90	2.87	3.34	363	361
3	5.80	3.29	4.02	362	360
4	8.71	4.83	3.74	362	359
5	11.61	5.65	3.85	361	358

The mass fraction burnt (MFB) is used to estimate the ignition delay and combustion duration to the amount of accumulated fuel or accumulated heat during the combustion period by the total fuel or total heat release [26]. The duration of 10%, 50%, and 90% MFB can be stated as (a) the point where the fuel injection starts and the point of ignition delay is the region for 10% MFB, (b) 50% MFB occurs when injected fuel is converted to heat energy, and (c) 10% to 90% MFB is the combustion duration [27]. From Fig. 13, the MFB for 10%, 50%, and 90% in PM is found to be lower than in baseline test. This is due to the combustion stability [8] within PM matrix, due to which the fuel burning rate progresses steadily.

HRR is a very significant combustion parameter, which is calculated by invoking the 1st law of thermodynamics using the in-cylinder gas pressure variables. Different phases of combustion are classified through HRR, namely, premixed, mixed phase and late combustion phase [28]. The variations of HRR with different combustion phases for PM and baseline test with the CA at part loads are shown in Fig. 14. In all the loads, the premix phase or the ignition delay is advanced up to 3°CA BTDC with PM than that of the baseline tests. With PM, it is found to be advanced till TDC. This advancement of premix phase with load increment indicated faster evaporation of charge with PM than in baseline test, i.e.,
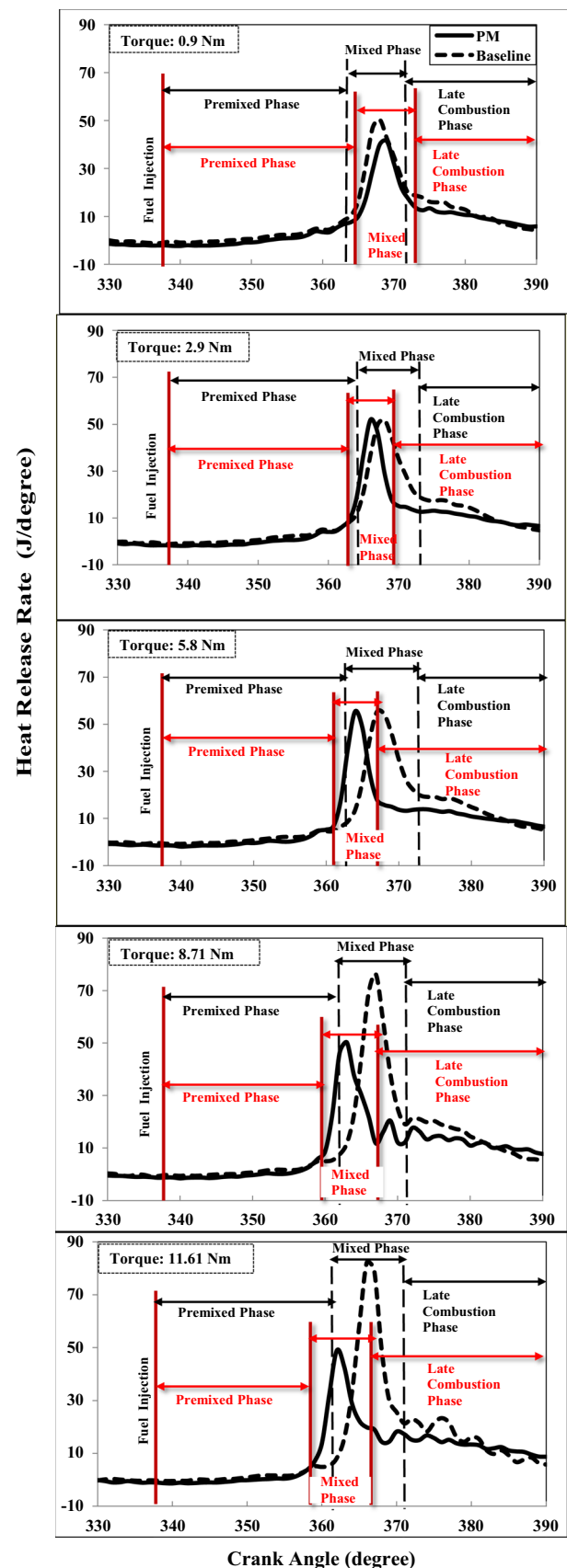

Fig. 14 Variation of HRR with CA at part load

Table 8 Variation of peak values of HRR with load

| Sl. no	Torque (Nm)	Peak values of HRR (J/°)	
		Baseline	PM
1	0.9	50.35	41.34
2	2.90	51.77	52.01
3	5.80	55.33	55.47
4	8.71	76.22	50.22
5	11.61	82.11	48.88

Fig. 15 Variation of NO_X with load

efficient heat transfer between fuel and air. The mixed phase in the plot depicts the combustion duration which is also found to be reduced with PM. This reduction of combustion duration in PM is due to the effect of its ignition delay. The late combustion phase is the duration where the after burning of fuel charge occurs [23]. This duration is found to be enhanced with the increment of load in PM than in baseline test due to efficient turbulent mixing [24] of unburnt and partially burnt fuel with the air.

HRR is found to be lower in PM at (0.9, 8.71, 11.61) Nm to that of the baseline test. However, there is a slight increment in HRR at 2.90Nm and 5.80Nm. This enhancement of HRR at 2.90Nm and 5.80Nm with PM is the result of the accumulation of fuel which resulted in temperature rise. Whereas at 0.9, 8.71, and 11.61Nm, a lion's share of the generated energy is spent to the piston movement, to produce more power. For HRR at 2.90Nm and 5.80Nm, a part of energy is also spent in piston movement, but due to more heat produced, the energy accumulation at PM will be higher than the latter. Thus, the expense of energy is higher at those loads, than that at the lower loads, resulting in the decrement in HRR. The comparisons of peak values of HRR with baseline and PM are shown in Table 8.

3.4 Emissions

A diesel engine usually produces higher content of oxides of nitrogen and sulfur than petrol engine in addition to unburnt hydrocarbon and oxides of carbon during combustion. The foremost causes for the emissions are non-homogeneity in combustion, nitrogen dissociation and contamination in fuel and air [23]. The variations of NO_X, CO_2 and HC at part loads with baseline and PM are plotted in Figs. 15, 16 and 17.

With the increase in load, the NO_X emission reduced by 62.1, 50.5, 30.8, 55.3, and 57.7% and CO_2 emission dropped by 39.5, 12.3, 15.9, 26.6, and 10.4%. The decrement in NO_X in PM is attributed to the controlled combustion temperature inside the cylinder as reported in an earlier work of the same group of authors [24]. NO_X is a function of temperature. As the combustion occurs, there is high generation of heat resulting in high temperature.
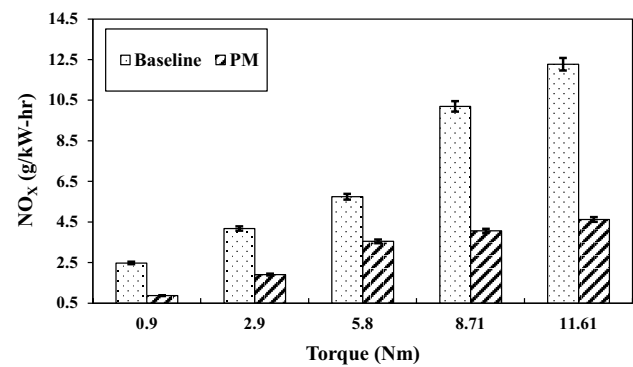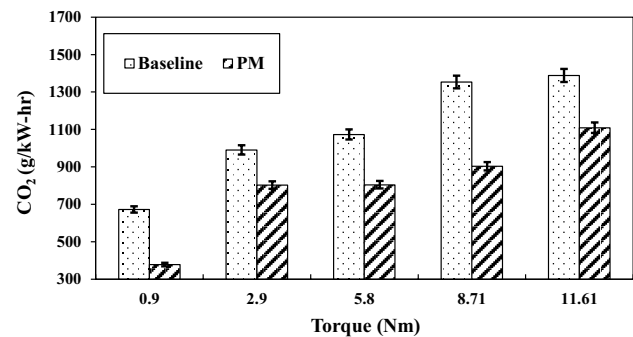
Fig. 16 Variation of CO_2 with load
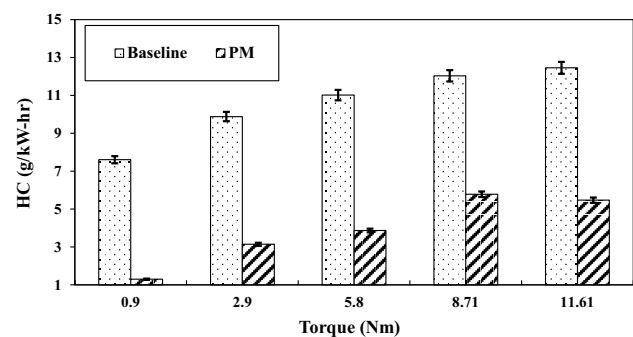
Fig. 17 Variation of HC with load

With the application of PM in diesel engine, the property of energy recuperation is activated [9], and hence the some portion of the heat generated from combustion is stored in the PM, owing to its high heat capacity. Moreover, the rate of heat transfer from the gases to the PM is improved by the high specific heat surface area provided by the matrix structure of the PM with high porosity. These factors contribute in keeping the maximum temperature of the combustible gases in check as compared to that of the baseline case. This is how combustion temperature is controlled

with the introduction of PM insert on the piston. The CO_2 formation with PM is observed to be lower than baseline test, owing to prompt evaporation of fuel as well as better oxidation of CO to CO_2.

The hydrocarbon (HC) emissions depend on the fuel components, combustion chamber geometry and engine operating parameters. The HC is formed because when fuel-rich mixture cannot react with enough quantity of oxygen. With lean mixture, the excess oxygen content leads to poor combustion resulting in HC emissions [23]. In this current work, the average HC emission reduction in PM is found to be 60% than in the baseline test. The variation of HC emissions with load for baseline test and PM is shown in Fig. 17. It is seen from the plot that the HC emission content increases with the increment in load for both the conditions. This is because with the increment in load, the pressure and temperature inside the cylinder increase leading to a higher burning rate. For baseline, the HC emission is higher due to inhomogeneity of the charge, whereas for PM, due to fuel-rich mixture and change in piston bowl geometry, the formation occurs. However, the potential to achieve homogeneity with PM leads to lower concentration of emissions than in baseline test.

4 Uncertainty analysis

The quantification of the instability of the output, owing to the variable input, is done using uncertainty analysis [29]. In the present work, sequential perturbation technique is considered to estimate the uncertainty of the parameters [30]. The parameters are air flow rate (1.2%), liquid fuel flow rate (0.2%), engine load (0.5%), engine speed (1.5%), etc. From the calculations, the accuracy of the performance and combustion is found to be within $\pm 3.9\%$. Also the accuracy for emission parameter is calculated to be $\pm 2.5\%$.

5 Conclusion

The experimental investigation by the application of SiC as ceramic PM on the modified piston bowl inside the compression ignition engine was performed. The results of the investigation were evaluated through the performance, combustion, and emission analysis, both with baseline and PM. The key outcomes of the investigation are summarized below:

(a) The performance parameter η_m with part load for PM was found to be augmented up to ~9% to that of the baseline test, and the values of BTHE were found a little lower than in baseline test.
(b) Further, with the use of PM it was found that the ignition delay got advanced by around 2°CA. This means

faster evaporation of fuel and efficient burning of the charge in comparison with baseline test. However, the average HRR dropped by around 21% with PM due to the regeneration effect.
(c) The characteristic features of PM have assisted in a significant reduction of engine out gases such as NO_X, CO_2 and HC. The average drop of NO_X, CO_2 and HC with load for PM was found to be around 62%, 39%, and 60%, respectively.

It has been observed from the experimental findings that the application of PM on the piston bowl in diesel engine has the potential to enhance the performance and control the engine-out gases. The current work was attempted at part load conditions and constant speed. However in the future, the work can also be extended for higher loads and at different speeds.

Appendix

Calculation of Height of the PM

Hemispherical piston bowl volume $= 36.81$ cc.

$$\Rightarrow V = \pi \times 2.6^2 \times \varphi \times L \tag{2}$$

where $L = 2.6$ cm.

Porosity of the PM

Machined cylindrical shape piston bowl volume $(r = h = 2.2$ cm$) = 46.7$ cc

$$\Rightarrow V = \pi \times r^2 \times h \tag{3}$$

Therefore, the minimum porosity applicable $= (36.81/46.7) = 78\%$ (for CR $= 17.5$).

References

1. Vigneswaran R, Annamalai K, Dhinesh B, Krishnamoorthy R (2018) Experimental investigation of unmodified diesel engine performance, combustion and emission with multipurpose additive along with water-in-diesel emulsion fuel. Energy Convers Manag 172:370–380. https://doi.org/10.1016/j.enconman.2018.07.039

2. Tesfa B, Mishra R, Gu F, Ball AD (2012) Water injection effects on the performance and emission characteristics of a CI engine operating with biodiesel. Renew Energy 37:333–344. https://doi.org/10.1016/j.renene.2011.06.035

3. Nadeem M, Rangkuti C, Anuar K, Haq MR, Tan IB, Shah SS (2006) Diesel engine performance and emission evaluation using emulsified fuels stabilized by conventional and gemini surfactants. Fuel 85:2111–2119. https://doi.org/10.1016/j.fuel.2006.03.013

4. Park CW, Kaviany M (2002) Evaporation-combustion affected by in-cylinder, reciprocating porous regenerator. J Heat Transfer 124(1):184–194. https://doi.org/10.1115/1.1418368

5. Mujeebu MA, Abdullah MZ, Bakar MZA, Mohamad AA, Abdullah MK (2009) A review of investigations on liquid fuel combustion in porous inert media. Prog Energy Combust Sci 35:216–230

6. Scheffler M, Colombo P (2006) Cellular ceramics: structure, manufacturing, properties and applications. Wiley, New York. https://doi.org/10.1002/3527606696

7. Weclas M (2004) Strategy for intelligent internal combustion engine with homogeneous combustion in cylinder. Sonderdruck Schriftenreihe University of Applied Sciences in Nuernberg. No. 261–14.

8. Trimis D, Durst F (1996) Combustion in a porous medium-advances and applications. Comb Sci Tech 121:153–168. https://doi.org/10.1080/00102209608935592

9. Mujeebu MA, Abdullah MZ, Abu Bakar MZ, Mohamad AA, Abdullah MK (2009) Applications of porous media combustion technology—a review. Appl Energy 86:1365–1375

10. Durst F, Weclas M (2001) A new type of internal combustion engine based on the porous-medium combustion technique. Proc Inst Mech Eng, Part D: J Auto Eng 215(1):63–81. https://doi.org/10.1243/0954407011525467

11. Hall MJ, Peroutka XN (1995) A porous media burner for reforming methanol for fuel cell powered electric vehicles. Society of Automotive Engineers International. Paper No. 950095

12. Reijnders J, Boot MD, Luijten CCM, Goey LPH, Frijters PJM (2009). Porous Fuel Air Mixing Enhancing Nozzle (PFAMEN), Society of Automotive Engineers. International Journal of Engines. Paper No. 2009-24-0028

13. Shahangian N, Honnery D, Ghojel J (2014) The role of porous media in homogenization of high pressure diesel fuel spray combustion. ASME J Energy Resources Technol 136:1–13

14. Pickenacker O, Pickenacker K, Wawrzinek K, Trimis D, Pritzkow WEC, Muller C, Goedtke P, Papenburg U, Adler J, Standke G, Heymer H, Tausher W, Jansen F (1999) Innovative ceramic materials for porous media burners, Interceram, Freiburg. Germany 48:424–433

15. Eltech ceramics private limited. Kurichi, Coimbatore, Tamil Nadu. https://www.eltechceramics.in/. Accessed 3 April 2018

16. Das S, Debnath BK, Das RS (2019) Effect on combustion behaviour in the presence of ceramic porous materials on the piston bowl of a diesel engine. In: Proceedings of the 25th national and 3rd international ISHMT-ASTFE. Heat and mass transfer conference. December 28–31, IIT Roorkee, India

17. Debnath BK, Saha UK, Sahoo N (2014) An experimental way of assessing the application potential of emulsified palm biodiesel toward alternative to diesel. J Eng Gas Turbines Power 136:1–12

18. Sarkar A (2018), Role of global fuel-air equivalence ratio and intake charge preheating in dual fuel diesel engines run on biogas and blended oxygenated pilot fuels. Dissertation, IIT Guwahati.

19. Ceratech product private limited.Gandhi road, Krishnagiri, Tamil Nadu, India. http://ceratech.in/. Accessed 10 April 2018

20. Savchenko N, Sevostyanova I, Sablina T, Gömze L, Kulkov S (2014) The influence of porosity on the elasticity and strength of alumina and zirconia ceramics. AIP Conf Proc 1623:547–550

21. Mishra VK (2016) Estimation of parameters in conduction radiation heat transfer in porous media. Dissertation, IIT Guwahati.

22. Heywood JB (1988) Internal combustion engine fundamentals, 1st edn. McGraw-Hill Education, New York

23. Ganesan V (2012) Internal combustion engine, 4th edn. McGraw-Hill Education, New Delhi

24. Das S, Debanth BK, Das RS, Stagni A, Faravelli T (2019) Numerical investigation of a porous media combustor in a small-scale compression ignition engine. Energy 186:115785. https://doi.org/10.1016/j.energy.2019.07.115

25. Agarwal AK, Gupta P, Dhar A (2015) Combustion, performance and emissions characteristics of a newly developed CRDI single cylinder diesel engine. Sadhana Indian Acad Sci 40:1937–1954

26. Agarwal AK, Dhar A, Gupta JG, Kim WI, Choi K, Lee CS, Park S (2015) Effect of fuel injection pressure and injection timing of Karanja biodiesel blends on fuel spray, engine performance, emissions and combustion characteristics. Energy Convers Manag 91:302–314

27. Cooney CP, Yeliana WJJ, Naber JD (2009) Combustion Characterization in an internal combustion engine with ethanol-gasoline blended fuels varying compression ratios and ignition timing. Energy Fuels 23:2319–2324

28. Ashok B, Nanthagopal K (2019) Eco friendly biofuels for CI engine applications. Advances in eco-fuels for sustainable environment, 1st edn. Woodhead Publishing, Cambridge, pp 407–440. https://doi.org/10.1016/C2017-0-04211-8

29. Geffray C, Gerschenfeld A, Kudinov P, Mickus I, Jeltsov M, Koop K, Grishchenko D, Pointer D (2019) Verification and validation and uncertainty quantification. Thermal hydraulic aspects of liquid metal cool reactors, 1st edn. Woodhead Publishing, Cambridge, pp 383–405. https://doi.org/10.1016/C2016-0-01216-0

30. Moffat RJ (1985) Using uncertainty analysis in planning of an experiment. ASME J Fluids Eng 107:173–178